FACTORS CONTROLLING OPEN-CIRCUIT VOLTAGE LOSSES IN ORGANIC SOLAR CELLS

Mohammed Azzouzi[1], Thomas Kirchartz[2,3] and Jenny Nelson[1]

[1]Department of Physics and Centre for Plastic Electronics, Imperial College London

[2]IEK-5 Photovoltaics, Forschungszentrum Jülich,

[3]Faculty of Engineering and CENIDE, Univ. of Duisburg-Essen, Carl-Benz-Str. 199, 47057 Duisburg, Germany.

ABSTRACT

The performance of solar cells based on molecular electronic materials is limited by relatively low open-circuit voltage relative to the absorption threshold. These voltage losses must be reduced to achieve competitive power-conversion efficiencies. Voltage losses are assigned to the molecular heterojunction required to dissociate photo-generated excitons and to relatively fast electron-hole recombination. Recent studies using luminescence have helped quantify these losses and understand their molecular origin. Recently, higher voltages and lower losses have been achieved using new molecular acceptors in place of traditional fullerenes, suggesting that optimizing chemical structure could enable improved device performance. This mini-review combines a device-physics perspective with a body of experimental observations to explore the practical and theoretical limits to V_{oc}.

HIGHLIGHTS

- Organic photovoltaic (OPV) devices traditionally show low open-circuit voltages (V_{oc}) relative to their optical absorption threshold, compared to other solar cell types.

- The large V_{oc} loss is assigned both to the need for a donor:acceptor heterojunction to split excitons, and to fast charge recombination.

- Recently, greatly reduced V_{oc} losses have been reported for OPV devices, especially when using non-fullerene acceptor materials.

- The voltage losses component due to 'charge separation' can be reduced to < 0.1 eV, sometimes without compromise to charge separation efficiency.

- The voltage losses component due to 'charge recombination' remains high and may be due to the soft and light nature of organic semiconductors.

- Analysing losses using luminescence to find the radiative limit seems the most reliable way to quantify V_{oc} losses.

- Understanding the origin of the non-radiative losses in OPV remains a target to establish the fundamental limit to efficiency.

V_{OC} LOSSES LIMIT THE EFFICIENCY OF OPV DEVICES

Over the past two decades, organic semiconductors have attracted significant interest as photoactive materials for solar energy conversion because they offer several key advantages such as ease of synthesis and processing, and tunability of properties. Their molecular nature, however, often constrains the materials' optoelectronic performance. In particular, (i) the localized and disordered nature of electronic states inhibits charge transport, demanding thin devices for efficient collection; and (ii) the localized nature of optically excited states (**excitons** (see Glossary)) together with low dielectric permittivity lead to a potential barrier opposing the dissociation of photogenerated excitons into independent charge pairs. The latter challenge is solved by blending electron-donating and electron-accepting components into a film, establishing a 'bulk heterojunction' where excitons are generated close to a donor:acceptor interface and dissociate via **charge transfer** at that interface (driven by the lower free energy of the charge-separated versus excitonic state) [1–3]. Photocurrent is then directed by embedding the blend layer between two electrodes of contrasting work-function. While the 'bulk heterojunction' approach leads to efficient light harvesting and high incident photon-to-current efficiency (or external quantum efficiency, EQE) [4], the interfacial energy step limits the achievable open-circuit voltage, V_{oc} (Box 1) especially when compared to the optical absorption threshold. As discussed below, V_{oc} appears to be further affected by relatively high rates of non-radiative charge recombination, potentially assisted by slow charge transport and large internal hetero-interface area. As a result, the so-called V_{oc} deficit (i.e., $E_g - qV_{oc}$, where E_g is the **optical band gap** and q is electronic charge) is seldom smaller than 0.6 eV in a working organic photovoltaic (OPV) device (compared with that of 0.4 eV in state-of-the-art inorganics) [5].

After appearing to stabilize around 11% in the early 2010s, the **power conversion efficiency** of organic solar cells advanced rapidly to reach 14% for single junction [6,7] and 17% for tandem cells [8] in 2018, approaching but still short of the record 22-26% efficiencies achieved by other semiconductors (e.g., Si, CIGS, CdTe, and perovskites) [9]. While early efficiency improvements were driven by novel donor polymers with improved properties such as a lower optical band gap (to benefit photocurrent), deeper

HOMO (to benefit voltage), and enhanced structural or transport properties [10], recent improvements reflect the availability of new high-performance molecular acceptor materials [11] (**non-fullerene acceptors**, NFAs) as alternatives to traditional fullerene-based acceptors. These new acceptors have been explored in ternary blend [12] and multijunction device configurations [8], enabling higher V_{oc} values. These developments, while promising, were driven in a largely empirical manner by availability of materials rather than by device-physics led design, and the practical and theoretical limits to V_{oc} are not yet understood. The question of what limits V_{oc} has recently stimulated a significant amount of research interest and is the focus of this review

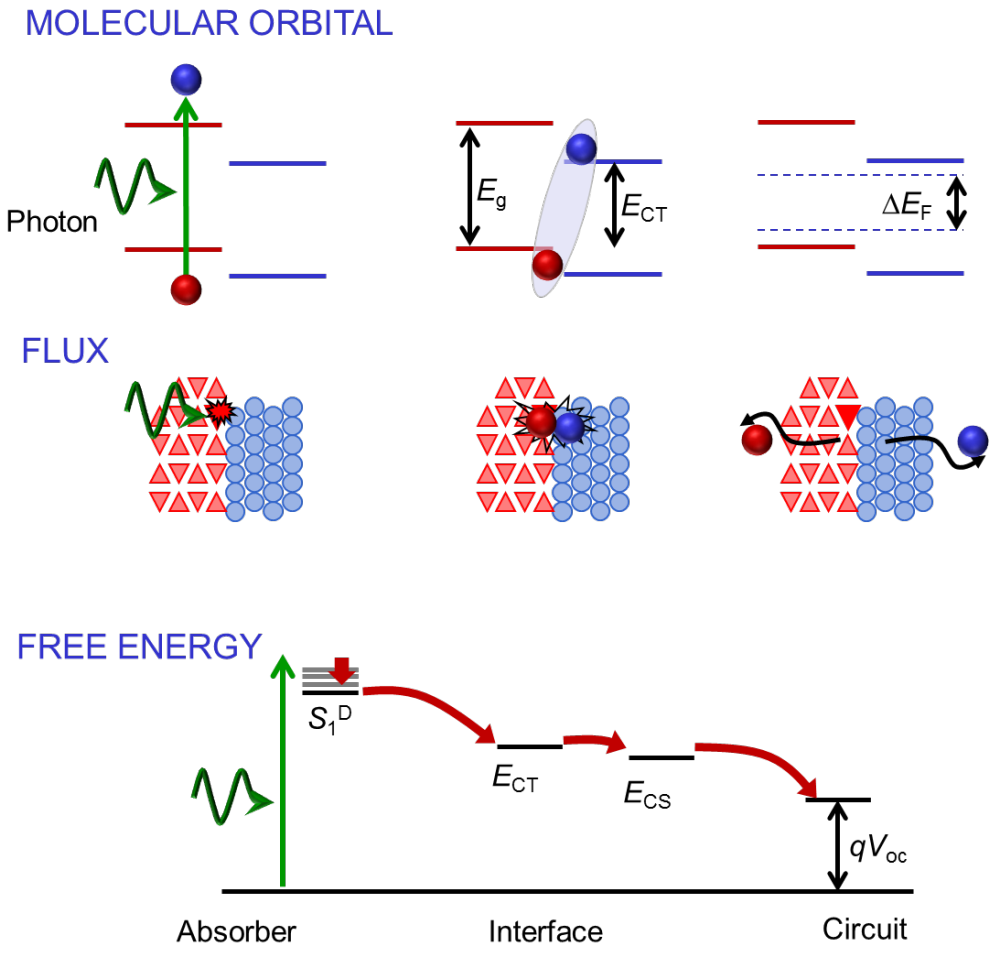

.

Figure 1. Key stages in photocurrent generation at an organic heterojunction. The charge generation process starts with a photon absorption and the excitation of a bound **exciton state** (left). This bound exciton needs to overcome the coulombic attraction to generate free charges. Introducing a donor:acceptor interface allows the electron and hole pair to be separated though a charge-transfer state (centre). The reduced free energy of the charge-transfer state relative to the exciton drives this electron transfer process. From the **Charge-transfer state** the electron and hole are further separated to form free charges that can travel towards the

electrodes (right) . The top panel shows the three stages in terms of **molecular orbitals**, the middle panel shows the flux of electrons on a schematic in real space, and the bottom panel shows the sequence in terms of free energy of the states involved. The right top-panel image shows the splitting of the quasi-Fermi energies of the two charge carrier populations after separation and thermal relaxation. This should be similar to qV_{oc} in the device at open circuit condition i.e when the photo-generation of free charge is balanced by the charge recombination. In the bottom panel, the difference between the energy of the charge-separated state (E_{CS}) and qV_{OC} is due to the recombination of the charges. In the figure, E_g represents the band gap energy, E_{CT} the energy of the CT state, ΔE_F the splitting of the quasi Fermi levels, S_1^D the singlet energy of the donor and E_{CS} the energy of the charge-separated state.

FACTORS CONTROLLING V_{OC}

Box 1. Relating open-circuit voltage to energy levels and recombination processes.

The open-circuit voltage is the difference between the quasi-Fermi levels at the two contacts in an illuminated solar cell at zero current flow. Figure 2a shows a band diagram of a generic (organic or inorganic) thin-film solar cell at open circuit. When photons are absorbed, excitons, and subsequently, electron-hole pairs are created. At open circuit, the only available process is electron-hole pair recombination. The open-circuit voltage is then the voltage where the volume-integrated generation and recombination rates of electron-hole pairs are equal. While the generation rate depends on photon flux but not on electron-hole concentrations, the recombination rate depends on the electron-hole concentrations. Different recombination mechanisms yield different concentration-dependent recombination rates. For simplicity, we consider bimolecular recombination that requires one electron and one hole for a single recombination event. In this case, the recombination rate, R, is given by

$$R = k_{\mathrm{bm}}\left(np - n_{\mathrm{i}}^2\right) \tag{1}$$

where k_{bm} is the bimolecular recombination coefficient (in units $\mathrm{cm^3 s^{-1}}$), np is the product of electron and hole densities, and n_{i} is the intrinsic carrier concentration. At open circuit, the average volumetric generation rate, G_{av}, of electron-hole pairs equals the average recombination rate, R_{av}. In the simplest approximation, np is assumed constant with position, implying that external voltage qV_{oc} is equal to the separation of the quasi-Fermi levels in the absorber volume. This is a reasonable approximation at open circuit for a thin absorber layer. Employing a Boltzmann approximation for the occupation of the states in the conduction and valence bands

$$np = N_{\mathrm{C}}N_{\mathrm{V}}\exp\left(\frac{qV_{\mathrm{oc}} - E_{\mathrm{g}}}{k_{\mathrm{B}}T}\right) = n_i^2\exp\left(\frac{qV_{\mathrm{oc}}}{k_{\mathrm{B}}T}\right) \tag{2}$$

where N_{C} and N_{V} are the effective densities of states for the conduction and valence bands, and E_{g} is the band gap. Thus,

$$G_{\mathrm{av}} = R(V_{\mathrm{oc}}) = k_{\mathrm{bm}}N_{\mathrm{C}}N_{\mathrm{V}}\exp\left(-\frac{E_{\mathrm{g}}}{k_{\mathrm{B}}T}\right)\left[\exp\left(\frac{qV_{\mathrm{oc}}}{k_{\mathrm{B}}T}\right) - 1\right] \tag{3}$$

At room temperature, for an efficient photovoltaic device $V_{oc} \gg \frac{k_B T}{q}$, which leads to $\exp(\frac{qV_{oc}}{k_B T}) \gg 1$ and a solution for V_{oc}

$$qV_{\mathrm{oc}} = E_{\mathrm{g}} - k_{\mathrm{B}}T\ln\left(\frac{k_{\mathrm{bm}}N_{\mathrm{C}}N_{\mathrm{V}}}{G_{\mathrm{av}}}\right). \tag{4}$$

By considering a perfect charge extraction at short circuit, $J_{\mathrm{sc}} = \int dx G_{\mathrm{av}}$ where the generation is integrated over device thickness from $x = 0$ to $x = d$. We define the saturation current density $J_0 = qk_{bm}n_i^2 d$, where n_i is the intrinsic density of states in the absorber. Therefore we can rewrite eq.4 (full derivation in reference [16])

$$V_{\mathrm{oc}} = \frac{n_{\mathrm{id}}k_{\mathrm{B}}T}{q}\ln\left(\frac{J_{\mathrm{sc}}}{J_0} + 1\right) \tag{5}$$

A device-physics perspective

OPV-device energetics are commonly considered in terms of the relative energies of donor and acceptor molecular orbitals and electrode work-functions. However, to fully understand the factors affecting V_{oc} it is necessary to take a device-physics perspective and consider the spatial distribution of charge density and recombination. Box 1 demonstrates that V_{oc} is determined by the energy difference between electron and hole levels, less an amount due to charge recombination.

Exciton separation in OPV devices requires use of a **heterojunction** (Figure 1). This donor:acceptor heterojunction may be planar or, more commonly, distributed throughout the absorber. Figure 2b illustrates a planar heterojunction for simplicity. The introduction of a heterojunction reduces the open-circuit voltage relative to that of a single absorber of the same optical gap. This becomes clear if we repeat the Box 1 derivation with $R = k_{\mathrm{bm}}\left(n_{\mathrm{acc}}p_{\mathrm{don}} - n_{\mathrm{i}}^2\right)$, where n_{acc} is the acceptor electron density and p_{don} the donor hole density, and allow N_{C} and N_{V} to represent the **effective density of states** of the acceptor conduction band and the donor valence band, respectively. Note that in a molecular semiconductor, the conduction and valence band energies can be replaced by the lowest unoccupied molecular orbital (LUMO) and highest unoccupied molecular orbital (HOMO) energies of the semiconductors. V_{oc} in Eq. 4 is now smaller for a given generation rate G_{av}, recombination coefficient k_{bm}, and material densities of states N_{C} and N_{V}, simply because the absorber gap E_{g} must be replaced by the **interfacial band gap** E_{i} shown in Figure 2b to yield

$$qV_{\mathrm{oc}} = E_{\mathrm{i}} - k_{\mathrm{B}}T\ln\left(\frac{k_{\mathrm{bm}}N_{\mathrm{C}}N_{\mathrm{V}}}{G_{\mathrm{av}}}\right) \tag{6}$$

Thus, the heterojunction reduces qV_{oc} by the interfacial energy offset, ($E_{\mathrm{g}} - E_{\mathrm{i}}$), for given absorber properties. Thus, tuning of interfacial energy levels is critical.

From Eq. 4 it is clear that higher values of the recombination coefficient k_{bm} reduce qV_{oc} relative to E_{i}. Importantly, assuming that E_i is weakly dependent on the temperature, Eq. 4 reveals a method to estimate E_{i} by measuring qV_{oc} as a function of temperature at constant G_{av} [13–15]. The zero-Kelvin limit of qV_{oc} should equal E_{i} in situations where interfacial recombination dominates.

To understand the dependence of qV_{oc} on light intensity, the dominant recombination mechanism in a given device must be known. While Eq. 5 assumes **bimolecular recombination**, a more general description of V_{oc} is given by [16]

$$V_{oc} = \frac{n_{id} k_B T}{q} \ln\left(\frac{J_{sc}}{J_0} + 1\right), \tag{7}$$

where n_{id} is the **ideality factor**, J_{sc} the short-circuit current density, and J_0 is the saturation current density. J_0 here represents the recombination current density in the cell at thermal equilibrium in the dark. Recombination mechanisms other than bimolecular recombination (e.g., recombination via localized states in the interfacial band gap or events at the absorber-electrode interfaces) exhibit different ideality factors, yielding distinct charge-density dependent penalties in V_{oc}. Thus, the reduction in V_{oc} below the limit imposed by the material's energy levels depends strongly on the recombination mechanism. For trap-mediated recombination, $1 < n_{id} < 2$ [17], while for absorber-electrode interface recombination, $0 < n_{id} \leq 1$ [18]. Thus, the dependence of V_{oc} on light intensity at constant temperature is frequently used to ascertain the dominant recombination mechanism [18].

The factors controlling V_{oc} in planar (as illustrated in Fig 2b) and bulk heterojunctions must be distinguished. In the planar organic heterojunction, qV_{oc} results from the directional charge-diffusion currents imposed by exciton dissociation at the heterojunction. Thus, a voltage will be detected irrespective of the electrode choice, although the device **fill factor** may be poor [19–21]. In the bulk heterojunction where both semiconductors contact both electrodes, contrast in contact work-functions is needed to direct the photocurrent and generate a voltage. Moreover, the anode and cathode work-functions should align with the donor HOMO and acceptor LUMO energies, respectively, to avoid recombination at these interfaces and loss in V_{oc}. Note that voltage losses from recombination at the electrodes are additional to donor:acceptor interface recombination and can be minimised through electrode choice [22,23].

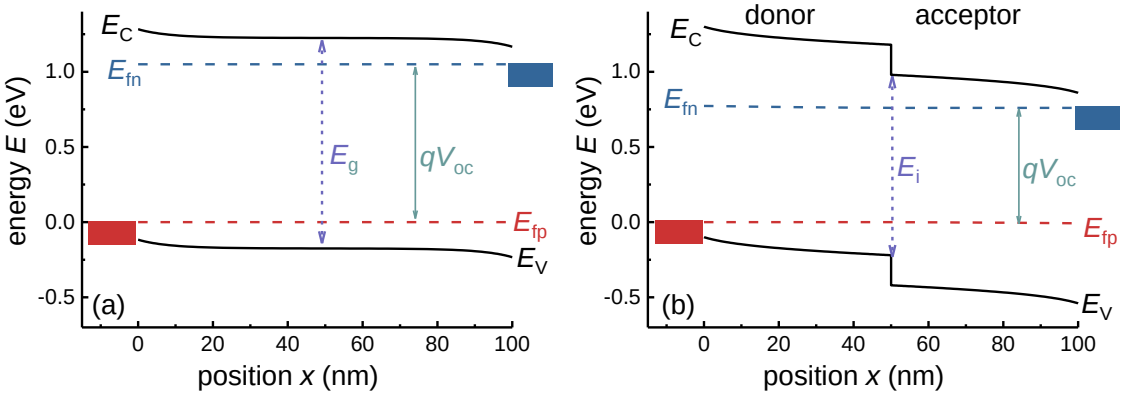

Figure 2. **Relation between V_{oc} and the energy levels in a solar cell.** (a) Band diagram of a solar cell at open circuit. The solar cell here consists of one semiconductor with conduction band edge (E_C) (equivalent to LUMO energy of a molecular semiconductor) and valence band edge (E_V) (equivalent to LUMO energy of a molecular semiconductor) separated by the band gap (E_g). The difference between the **quasi-Fermi levels**, E_{fn} at the cathode ($x = d$) and E_{fp} at the anode ($x = 0$) is the open circuit voltage qV_{oc}. In the example shown, this difference of Fermi levels at the contacts is almost identical to the Fermi level separation at any point in the device. (b) Band diagram of a heterojunction solar cell at open circuit. Now recombination at the donor:acceptor interface with interfacial band gap (E_i) limits V_{oc}. Organic solar cells typically consist of a blend of donor and acceptor molecules leading to a high density of heterojunctions like that shown in panel (b). The red and blue rectangles indicate the anode and cathode Fermi levels, respectively.

Theoretical limits to V_{oc}

The maximum achievable value of V_{oc} in a solar cell is controlled by the interfacial energy gap and parameters controlling recombination for the dominant mechanism (e.g., minimum k_{bm} values for bimolecular recombination). The only thermodynamically necessary source of recombination in a solar cell is radiative recombination because absence of radiative recombination implies absence of absorption (from detailed balance) [24]. Thus, one may define a radiative saturation current density

$$J_{0,\mathrm{rad}} = qp_{\mathrm{e}}k_{\mathrm{rad}}n_{\mathrm{i}}^2 d \tag{8}$$

where p_e is the photon emission probability [25] and k_{rad} the bimolecular recombination coefficient. It is straightforward to then define a **radiative open-circuit voltage**

$$qV_{\mathrm{oc,rad}} = kT\ln\left(\frac{J_{\mathrm{sc}}}{J_{0,\mathrm{rad}}}+1\right) = E_{\mathrm{i}} - kT\ln\left(\frac{p_{\mathrm{e}}k_{\mathrm{rad}}N_{\mathrm{C}}N_{\mathrm{V}}}{G_{\mathrm{av}}}\right) \tag{9}$$

The radiative open-circuit voltage can be determined experimentally using a combination of solar cell **quantum-efficiency measurements** and **electroluminescence spectroscopy** as discussed elsewhere [26]. The actual open-circuit voltage (V_{oc}) can then be related to $V_{oc,rad}$ by [27–29]

$$qV_{oc} = kT \ln\left(\frac{J_{sc}}{J_0}\right) = qV_{oc,rad} + kT \ln\left(Q_e^{lum}\right) \quad (10)$$

where Q_e^{lum} is the solar cell **external luminescence quantum efficiency**. Thus, luminescence measurements can be used to quantify how close the device approaches its thermodynamic limit in open-circuit voltage. Typical values for Q_e^{lum} in OPV devices, and the corresponding voltage loss $\frac{kT}{q}\ln\left(Q_e^{lum}\right)$, are in the range of 10^{-7} to 10^{-4} [30–32].

Empirical Correlations

Organic solar cells with a single semiconductor layer contacted with electrodes of sufficiently contrasting work-functions exhibit high qV_{oc} values related to the semiconductor band gap but afford low photocurrents (at least for polymers) due to poor charge separation. When a second (acceptor or donor) component is added to promote charge separation, the interfacial gap overrides the absorber gap in controlling electron and hole **quasi-Fermi levels**, and V_{oc} quickly diminishes (figure 2b) [33,34]. Since the heterojunction interfacial gap, E_i, can be approximated by the difference in energies of the donor HOMO and acceptor LUMO (i.e., $E_i = E_{L,A} - E_{H,D}$), qV_{oc} should be correlated to this energy difference (assuming that the recombination mechanism and associated parameters are conserved). Such correlation has been observed by several groups for polymer:fullerene blend devices (see Figure 3a) varying the polymer [35] or fullerene [22,36], as well for polymer:metal oxide systems [37]. However, qV_{oc} is lower than E_i by several tenths of an eV indicating significant losses to recombination [35].

It is important to isolate the effects of recombination at contacts to understand the V_{oc} limit. Early studies established that while photogeneration at a planar heterojunction always generates a photovoltage [20], insufficiently low cathode (or insufficiently high anode) work-functions in a bulk heterojunction result in recombination of holes at the cathode (or electrons at the anode) and pinning of the

charge carrier quasi-Fermi levels to the electrode work function, thus limiting V_{oc} [36]. This electrode-driven limitation to V_{oc} can be reduced by modifying contact work-functions, choice of metal [22], use of doped [21] or dielectric interlayers [39], and/or by treatment of interlayers to control work-functions [40].

Recently, several groups have attempted to explain the difference between qV_{oc} and E_i through differences in the dominant recombination processes for the typical case where recombination occurs predominantly at the donor:acceptor interface. Maurano and colleagues showed that measured V_{oc} values agreed more closely with Eq. 5 (Figure 3b) when the bimolecular recombination term in Eq. 5 for polymer:fullerene blends was estimated using experimentally measured k_{bm} values than when differences in recombination rate were neglected [41]. Other workers reported a correlation between the quantity assigned to recombination (i.e., E_i - qV_{oc}) and the reciprocal of the dielectric permittivity of the medium [42,43]. This correlation is rationalized by considering a Langevin-type recombination mechanism where the probability of electron-hole encounters is dependent on their Coulombic interaction. Some studies showed that the recombination-related V_{oc} loss could be correlated to the blend microstructure, specifically, the donor:acceptor interface area (since recombination flux should increase with increasing interfacial area) [42]. The magnitude of the recombination term can also be related to the extension of tails of states into the band gap, given that greater disorder would limit V_{oc} at low charge-carrier densities [40]. However, a shared limitation of many empirical studies is that the interfacial energy gap is estimated, typically from information on the isolated semiconductor HOMO and LUMO energies, and not directly determined for the studied systems.

Ternary-blend systems consisting of one donor and two acceptors, or two donors and one acceptor, introduce additional control over $V_{oc.}$ While simple models suggest that V_{oc} is limited by the smaller of the two possible interfacial gaps in a ternary system, experiments revealed that increasing the concentration of the component with the larger E_i increased V_{oc}. This was assigned to sampling by extended electronic states of a continuously changing effective medium [45], and, in one case, to the ability of the additional component to disrupt crystallinity, and hence energy levels of the blend, as well as to an unequal concentration of acceptor molecules around the donor [12]. The recent availability of a wide range of molecular acceptors has increased the possibilities for optimizing ternary systems to enhance photocurrent and limit recombination.

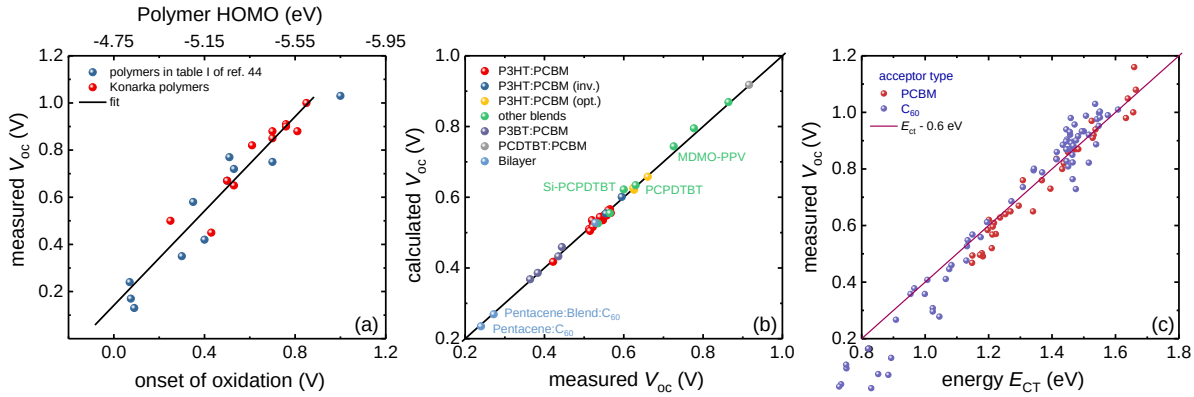

Figure 3. Examples of attempts to correlate V_{oc} with energy levels and additional correction terms. (a) Data from Scharber et al. [46] showing that qV_{oc} correlates with the polymer HOMO energy in polymer/fullerene systems (all with a common acceptor LUMO), and accordingly, with the $\boldsymbol{E_{L,A} - E_{H,D}}$ gap; (b) data [41] showing that qV_{oc} correlates with the $\boldsymbol{E_{L,A} - E_{H,D}}$ gap with a semi-empirical correction for recombination; and (c) data [47] showing that qV_{oc} correlates with the charge-transfer state energy monitored using electroluminescence.

METHODS FOR QUANTIFYING V_{OC} LOSSES

Voltage losses in OPV devices are typically quantified by the difference of qV_{oc} relative to the onset of optical absorption (i.e., $E_g - qV_{oc}$) [48,49] or to the interfacial energy gap (i.e., $E_i - qV_{oc} = E_{L,A} - E_{H,D} - qV_{oc}$). Both metrics for voltage loss are problematic due to uncertainties in the relevant energies, making it difficult to establish clear underlying relationships. The first quantity relies on precise measurement of the absorber band gap which requires knowledge of the density of states near the band edges and a proper definition of the band gap for a disordered material [5]. As discussed elsewhere [5], there are several ways to quantify the band gap for organic devices, for example, by considering the absorption onset, absorption edge, or shape of the absorption tail. Different definitions lead to voltage-loss values that can differ by more than 0.1 V. The second quantity where qV_{oc} is compared to E_i [35] relies on knowledge of the HOMO and LUMO energies in similar conditions to those within the heterojunction device. HOMO and LUMO values will be affected by the material state (solid or solution), degree of crystallinity, interfacial dipoles, in addition to the measurement and analysis method. The large disparity

between reported values for similar materials already indicates that this quantity is difficult to quantify, and so it cannot be used predictively.

The spectroscopic observation of sub-gap charge-transfer states in absorption and, importantly, emission spectroscopy [13,50–52] brought a means to measure the E_i since E_i is approximately equal to E_{CT}, the energy relative to ground of the charge-transfer (CT) state which is populated by interfacial charge transfer and can interact weakly with light. The precise determination of E_{CT} using electroluminescence [31,51] led the community to consider E_{CT} a more reliable approximation to the upper limit for qV_{oc} (Figure 3c) and to use E_{CT} - qV_{oc} as a preferred metric to quantify voltage losses due to recombination. By comparing the extrapolated temperature dependent V_{oc}(T) and $E_{CT}(T)$ at zero Kelvin, Vandewal and co-workers showed that V_{oc} for several polymer:fullerene systems is indeed limited by E_{CT} [13,53]. Moreover, by applying **the principle of reciprocity** to the optical absorption and emission of the charge-transfer states, Vandewal and co-workers distinguished a V_{oc}-loss term related to radiative properties of the CT state, from a non-radiative loss related to the **luminescent quantum efficiency** Q_e^{lum} of the cell (similar to Eq. 9). The approach was further generalized, without assuming Gaussian spectral forms for emission and absorption, by Yao and colleagues who quantified the radiative limit $V_{oc,rad}$ from the high-dynamic-range EQE of the device extended to lower photon energies using measured EL spectra and assuming the reciprocity of EQE and EL [30] (Figure 4a). The composite spectrum is then used to quantify excess non-radiative losses $\Delta V_{oc,nrad}$ by comparing it to measured V_{oc} in standard solar irradiance, while a loss related to the shape of the CT absorption spectrum $\Delta V_{oc,abs}$ is extracted as $V_{oc,SQ} - V_{oc,rad}$ (Figure 4b).

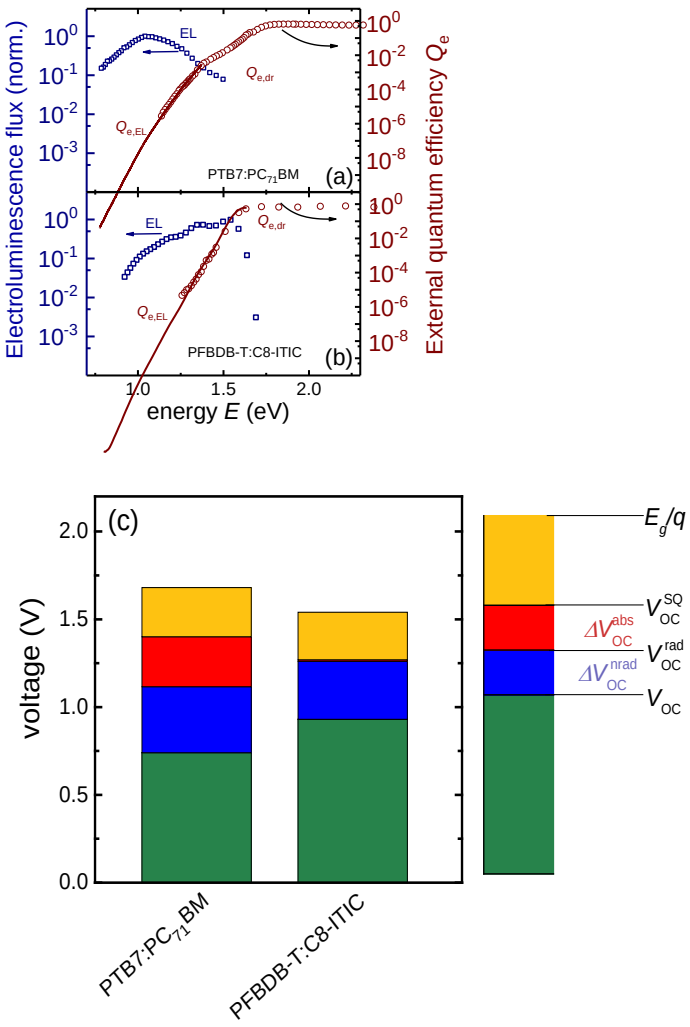

Figure 4. Correlating V_{oc} with properties derived from luminescence spectra. (a, b) Electroluminescence and external-quantum-efficiency spectra for devices from two different material combinations, (a) PTB7:PC$_{71}$BM [30] (a fullerene acceptor), and (b) PFBDB-T:C8-ITIC [54] (a small molecule acceptor-donor-acceptor acceptor) which shows a steep absorption onset; (c) a bar chart of voltage losses divided into 3 contributions: $\boldsymbol{E_g - V_{oc,SQ}}$ which is unavoidable, $\boldsymbol{\Delta V_{oc,abs}}$ which is the **excess loss due to the non-sharp absorption onset**, and $\boldsymbol{\Delta V_{oc,nrad}}$ which is the non-radiative loss [55].

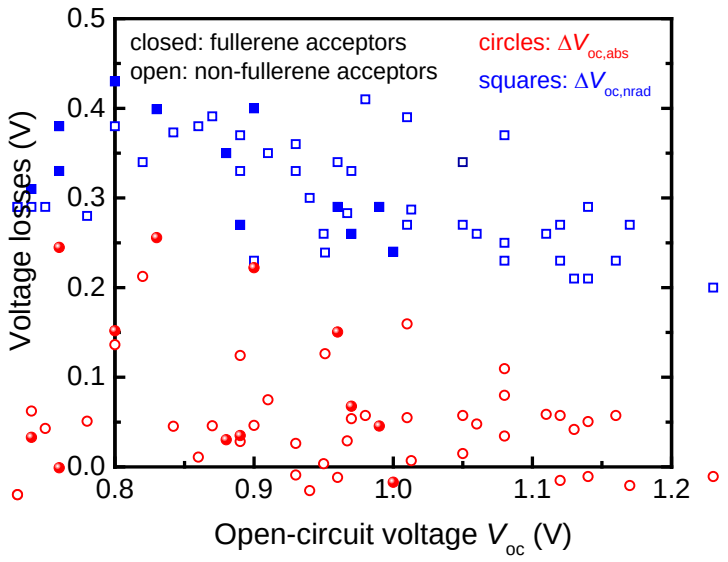

Figure 5. Typical range of different voltage losses in organic solar cells. Absorption onset voltage losses (red circles) and non-radiative voltage losses (blue squares) as a function of V_{oc} for some recent OPV devices [32,48,56–70]. Most high V_{oc} values are achieved with non-fullerene acceptors. Note that the losses due to a smeared out absorption onset have historically been large in some polymer:fullerene blends (P3HT:PCBM is an example) but are nearly negligible in some of the best blends involving non-fullerene and even some fullerene acceptors. Thus, in many of the more recent blends, the loss due to **non-radiative recombination** is the dominant one. This loss has been reduced in the past to ~250 mV but not substantially below this value.

KEY DEVELOPMENTS IN REDUCING V_{OC} LOSSES

Figure 5 displays a plot of voltage losses as a function of V_{oc} for some of the most recently published OPV devices [27, 29]. Here, the absorption onset is calculated using the reported band gap. Unfortunately, differences in the band-gap definition could result in errors of up to 0.1 V. First, we note that most devices with V_{oc} over 1 V were fabricated using non-fullerene acceptors. Second, it is clear from the plot that absorption onset losses can be reduced to values of order 0.01 eV, whereas the non-radiative part is still significant. These losses have evolved differently considering that early fullerene-based OPV devices often showed absorption onset loses of over 0.5 eV [27].

Reducing OPV absorption-onset voltage losses

The absorption-related voltage loss, $\Delta V_{oc,abs}$ (defined as the difference between the **Shockley-Queisser voltage limit** [71] for the particular band gap and $qV_{oc,rad}$), has decreased steadily with new material development, especially following the established design rule for high V_{oc} that $E_{D,H}$ -$E_{A,L}$ should be maximized for a given optical gap [27,32]. Recently, $V_{oc,rad}$ has been increased further through the development of new donor and acceptor materials [47,54,75,76] that combine electron-rich and electron-poor moieties in low molecular-weight, processable oligomers to offer precise control over optical gap, HOMO and LUMO energies and microstructure, affording smaller interfacial offsets. The trend in $V_{oc,rad}$ has also followed improved understanding of the significance of the charge-transfer-state optical properties from both experimental [74–76] and theoretical [77,78] perspectives. Notable improvement routes are reducing the HOMO or LUMO offset between the donor and acceptor, thus making the CT absorption steeper, and/or optimizing the interface microstructure to enhance CT state properties [82–84]. As a result, most high-efficiency devices today show a sharp absorption turn-on that reduces $\Delta V_{oc,abs,}$ and brings $V_{oc,rad}$ closer to $V_{oc,SQ}$ [85].

Reducing ***non-radiative voltage losses***

Unlike the absorption-onset voltage loss ($\Delta V_{oc,abs}$), the non-radiative voltage loss ($\Delta V_{oc,nrad}$) is still significant for most OPV devices (i.e., ~0.3-0.4 V). This loss compares unfavourably with state-of-the-art silicon (0.2 eV) and perovskite (0.1 eV) devices [30,83]. Nevertheless, several OPV devices have reached values as low as 0.23 V [56,69,82]. Unfortunately, the molecular origins of $\Delta V_{oc,nrad}$ are not yet well understood for OPVs. Historically, **non-radiative recombination** in OPV devices has been related to a diffusion-limited recombination process, where the rate-limiting factor is finding the respective recombination partner and not the dissipation of the energy of the electron-hole pair by exciting molecular vibrations [84–86]. However, poor correlation of observed recombination dynamics and model parameters rendered this model unsuitable for predicting voltage losses [65]. Recent work has introduced a mechanistic model for recombination, wherein radiative and non-radiative recombination both occur at the donor:acceptor interface via the relaxation of a charge-transfer excited state to the ground state (Figure 6a). Within this framework, the properties of the charge-transfer state affect $\Delta V_{oc,nrad}$ [47,87,88]. While the wide spacing of vibrational modes in carbon-based materials appears to enhance non-radiative decay,

increasing non-radiative loss for low energy-gap systems (a manifestation of the 'energy gap law' [89]), the approach also suggests approaches for reducing $\Delta V_{\mathrm{oc,nrad}}$. Figure 6b shows how particular charge-transfer state properties affect $\Delta V_{\mathrm{oc,nrad}}$ and $V_{\mathrm{oc,rad}}$ within the model of Ref. 84. These models still neglect several important blend-film properties such as energetic disorder, microstructure, and recombination away from the donor:acceptor interface (e.g., at electrodes) [90,91]. Nonetheless, these models highlight several design rules to improve the overall V_{oc}, such as using materials with a high luminescence efficiency for the CT state, which requires high luminescence in both the donor and the acceptor as stressed by Qian and colleagues [69].

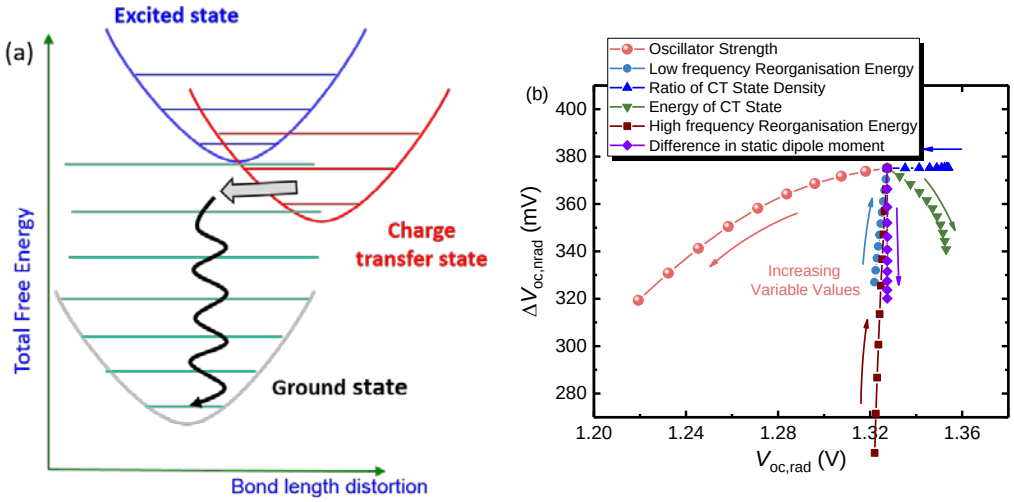

Figure 6. Model of non-radiative recombination via a charge-transfer state. (a) A sketch of potential-energy surfaces for the excited, charge-transfer (CT), and ground states of a donor:acceptor complex. Shown is a non-radiative decay process where energy transfer from the CT state to a high vibronic mode of the ground state is followed by decay via several vibronic modes (horizontal lines); and (b) calculated effect of varying charge-transfer state properties on the radiative and non-radiative voltage losses. Adapted from [87].

Relationships between V_{oc}, charge-separation efficiency, and fill factor

One of the most intriguing recent developments in OPVs is efficient photocurrent generation in systems where the interfacial gap and lowest single-component optical gap are nearly identical. Historically, it was accepted (and observed in fullerene systems) that a significant heterojunction energetic offset was needed to dissociate the exciton into independent charges [92,93], and that this offset limited both the voltage and overall efficiency of OPV devices. This perspective is based on the view that the

interfacial offset can provide the energy for a closely bound charge pair to overcome its Coulombic binding energy. However, several recent reports (often based on non-fullerene acceptors) suggest that low offset and high V_{oc} need not impose any penalty on charge-generation efficiency [69,94,95]. Moreover, photocurrent was generated efficiently by direct excitation of CT states even in high offset systems [81], suggesting that charge pairs do not necessarily encounter a barrier to separation. The observed insensitivity of the charge generation efficiency to the interfacial offset can be rationalized in several ways: (1) in terms of excitations populating an ensemble of excited states, some of which are well delocalized across the interface [96]; (2) by an entropic contribution that helps to reduce the free energy of charge-separated states relative to that of the originating charge-transfer states [97]; or (3) by microstructural gradients that stabilize more separated pairs. The notion that low offsets do not necessarily impede charge separation is supported by Figure 7a which shows that the maximum value for EQE ($EQE_{\max}$) is not strongly correlated to the optical gap-qV_{oc} difference. This suggests that there is no intrinsic limitation to achieving efficient charge separation for qV_{oc} close to the optical gap. However, when plotted against $\Delta V_{oc,nrad}$, both EQE_{max} and the device fill factor are limited for low non-radiative losses (Figure 7b and 7c). The fill factor for $V_{oc} > 1\,V$ appears to be limited to 65% despite the fact that leading OPV device fill factors are around 80% [102]. This observation questions whether reducing the interfacial offset in OPV devices affects the recombination mechanism in such a way that it limits the achievable fill factor, noting that recombination mechanisms with different **ideality factor** lead to a different fill factor.

Low V_{oc} losses and high V_{oc} can result when the interfacial offset is low, and for this to translate into high efficiency, the charge separation efficiency must be high under operating conditions. Currently, there is no agreed microscopic picture relating interfacial charge separation, charge recombination mechanism, and interfacial offset. However, observations of the temperature dependence of V_{oc} and charge-separation dynamics in these low-offset systems may offer insight. Qian and co-workers observe that the dynamics of charge-pair formation becomes slow (hundreds of ps rather than sub-ps for traditional OPV systems) in systems of low interfacial offset [69]. This is reminiscent of dye-sensitised solar cells where optimized systems exhibit charge separation slightly faster than excited-state decay [99]. Gao and co-workers also observed that V_{oc} does not monotonically increase with reducing temperature as suggested by Eq. 4. Rather, V_{oc} decreases sharply at low temperature in lower offset systems, suggesting that charge separation becomes compromised [104]. The relationship between interfacial charge separation and charge

recombination involves the same molecules but different pairs of states (excited-to-CT compared with CT-to-ground). Thus, the specific molecular geometry and excited-state symmetry can, potentially, be exploited to control the balance of charge-transfer processes [101]. These observations suggest that it is critical to understand the impact of interfacial offset on the balance of charge separation and recombination kinetics to optimize the performance of low-interfacial-offset systems and minimize voltage losses.

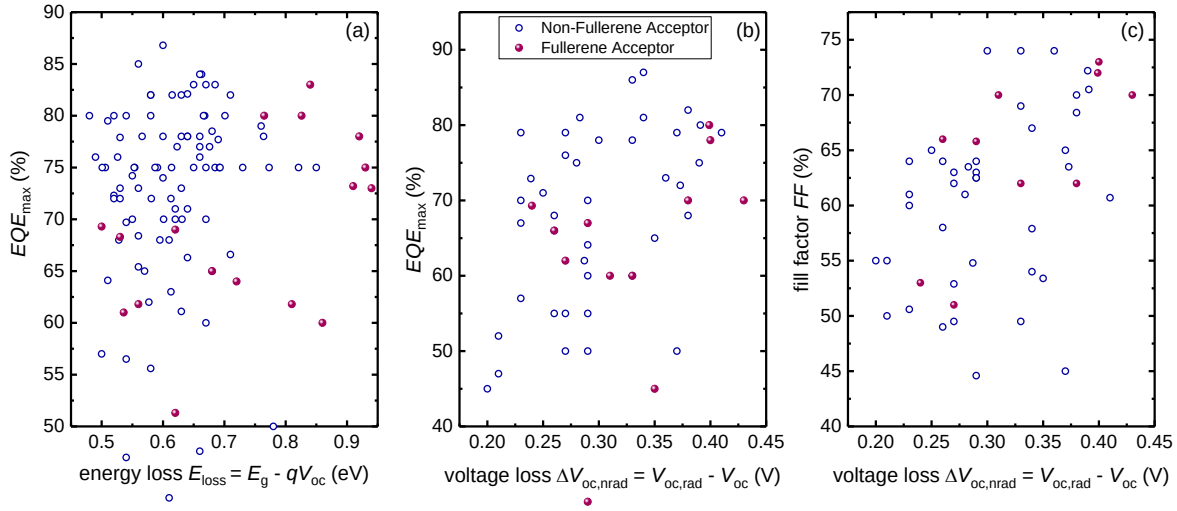

Figure 7. **Quantifying the compromise between charge collection and V_{oc}.** The graph always shows a comparison between one figure of merit for charge collection (either EQE_{max} or the *FF*) as a function of one figure of merit for the losses in V_{oc}. (a) EQE_{max} against voltage deficit relative to the absorber band gap; (b) EQE_{max} against $\Delta V_{oc,nrad}$ and (c) *FF* against $\Delta V_{oc,nrad}$ *for* different devices [32,48,56–70]. The data shows that efficient charge collection at short circuit is possible for energy losses $E_g - qV_{oc} \sim 0.5$ eV and $V_{oc,rad} - V_{oc} \sim 0.25$ V but not below. This is substantially better than what is possible with most fullerene-based acceptors but still less than what is possible with some inorganic solar cell materials. So far there are almost no examples of devices that combine low voltage losses with high *FF* (cf. panel c).

CONCLUDING REMARKS

Understanding the factors controlling open-circuit voltage in organic heterojunction solar cells remains a key major challenge to their scientific and technological mastery (see Outstanding Questions). Over the last two decades, a growing body of data for diverse material combinations, along with improved experimental probes, have helped develop a picture of the factors limiting V_{oc}. While qV_{oc} increases with increasing energy gap between the donor HOMO and acceptor LUMO, it is not yet clear how close it can approach the limit of that HOMO-LUMO gap. Main voltage losses are assigned to the cost of dissociating

the photogenerated exciton into a charge pair at the donor:acceptor heterojunction and to the non-radiative recombination of separated charges. Surprisingly, recent studies (often using non-fullerene acceptors) have shown that charge separation can occur with very low apparent driving forces. In contrast, the voltage loss due to non-radiative recombination remains rather high at ~0.25-0.4 eV (compared with <0.2 eV for inorganic solar cells). This has been related to efficient energy dissipation by high-energy vibrational modes of the carbon-based materials. Nevertheless, the diversity in potential chemical structures, enabled by recently developed conjugated molecular acceptors and new mechanistic models, opens the way to determining the underlying molecular mechanisms and further reducing losses.

Acknowledgments

M.A thanks the UK Engineering and Physical Sciences Research Council (ESPRC) for a postgraduate studentship. J.N. acknowledges funding from the EPSRC (grant numbers EP/P005543/1, EP/M025020/1), the EPSRC Supersolar Hub (EP/P02484X/1), and the European Research Council under the European Union's Horizon 2020 research and innovation program (grant agreement No 742708). T.K. acknowledges support from the DFG (Grant KI-1571/2-1). The authors thank Flurin Eisner for his help in collecting data, Markus Scharber for providing the original data shown in Fig. 3a and Dan Credgington for providing the original data shown in Fig. 3b.

REFERENCES

[1] N. S. Sariciftci, L. Smilowitz, A. J. Heeger, F. Wudl, and A. J. Heeger, *Photoinduced electron transfer from a conducting polymer to buckminsterfullerene.*, Science **258**, 1474 (1992).

[2] G. Yu, J. Gao, J. C. Hummelen, F. Wudl, and A. J. Heeger, *Polymer Photovoltaic Cells: Enhanced Efficiencies via a Network of Internal Donor-Acceptor Heterojunctions*, Science (80-.). **270**, 1789 (1995).

[3] J. J. M. Halls, C. A. Walsh, N. C. Greenham, E. A. Marseglia, R. H. Friend, S. C. Moratti, and A. B. Holmes, *Efficient photodiodes from interpenetrating polymer networks*, Nature **376**, 498 (1995).

[4] D. Baran, N. Gasparini, A. Wadsworth, C. H. Tan, N. Wehbe, X. Song, Z. Hamid, W. Zhang, M. Neophytou, T. Kirchartz, C. J. Brabec, J. R. Durrant, and I. McCulloch, *Robust nonfullerene solar cells approaching unity external quantum efficiency enabled by suppression of geminate recombination*, Nat. Commun. **9**, 2059 (2018).

[5] Y. Wang, D. Qian, Y. Cui, H. Zhang, J. Hou, K. Vandewal, T. Kirchartz, and F. Gao, *Optical Gaps of Organic Solar Cells as a Reference for Comparing Voltage Losses*, Adv. Energy Mater. **1801352**, 1 (2018).

[6] S. Zhang, Y. Qin, J. Zhu, and J. Hou, *Over 14% Efficiency in Polymer Solar Cells Enabled by a Chlorinated Polymer Donor*, Adv. Mater. **30**, 1 (2018).

[7] W. Li, L. Ye, S. Li, H. Yao, H. Ade, and J. Hou, *A High-Efficiency Organic Solar Cell Enabled by the Strong Intramolecular Electron Push–Pull Effect of the Nonfullerene Acceptor*, Adv. Mater. **1707170**, 1 (2018).

[8] L. Meng, Y. Zhang, X. Wan, C. Li, X. Zhang, Y. Wang, X. Ke, Z. Xiao, L. Ding, R. Xia, H.-L. Yip, Y. Cao, and Y. Chen, *Organic and solution-processed tandem solar cells with 17.3% efficiency*, *Organic*

and Solution-Processed Tandem Solar Cells with 17.3% Efficiency (n.d.).
[9] Y. Hishikawa, W. Warta, M. A. Green, D. H. Levi, J. Hohl, E. Anita, W. Y. H. Baillie, and E. D. Dunlop, *Solar cell efficiency tables (version 50)*, 668 (2017).
[10] K. Alberi, M. B. Nardelli, A. Zakutayev, L. Mitas, S. Curtarolo, A. Jain, M. Fornari, N. Marzari, I. Takeuchi, M. L. Green, M. Kanatzidis, M. F. Toney, S. Butenko, B. Meredig, S. Lany, U. Kattner, A. Davydov, E. S. Toberer, V. Stevanovic, A. Walsh, N.-G. Park, A. Aspuru-Guzik, D. P. Tabor, J. Nelson, J. Murphy, A. Setlur, J. Gregoire, H. Li, R. Xiao, A. Ludwig, L. W. Martin, A. M. Rappe, S.-H. Wei, and J. Perkins, *The 2019 materials by design roadmap*, J. Phys. D. Appl. Phys. **52**, 013001 (2019).
[11] C. Yan, S. Barlow, Z. Wang, H. Yan, A. K. Y. Jen, S. R. Marder, and X. Zhan, *Non-fullerene acceptors for organic solar cells*, Nat. Rev. Mater. **3**, 18003 (2018).
[12] D. Baran, R. S. Ashraf, D. A. Hanifi, M. Abdelsamie, N. Gasparini, J. A. Röhr, S. Holliday, A. Wadsworth, S. Lockett, M. Neophytou, C. J. M. Emmott, J. Nelson, C. J. Brabec, A. Amassian, A. Salleo, T. Kirchartz, J. R. Durrant, and I. McCulloch, *Reducing the efficiency–stability–cost gap of organic photovoltaics with highly efficient and stable small molecule acceptor ternary solar cells*, Nat. Mater. **16**, 363 (2017).
[13] K. Vandewal, K. Tvingstedt, A. Gadisa, O. Inganäs, and J. V. Manca, *Relating the open-circuit voltage to interface molecular properties of donor:acceptor bulk heterojunction solar cells*, Phys. Rev. B - Condens. Matter Mater. Phys. **81**, 1 (2010).
[14] M. Turcu, O. Pakma, and U. Rau, *Interdependence of absorber composition and recombination mechanism in Cu(In,Ga)(Se,S)2 heterojunction solar cells*, Appl. Phys. Lett. **80**, 2598 (2002).
[15] B. P. Rand, D. P. Burk, and S. R. Forrest, *Offset energies at organic semiconductor heterojunctions and their influence on the open-circuit voltage of thin-film solar cells*, Phys. Rev. B **75**, 115327 (2007).
[16] J. Nelson, *The Physics of Solar Cells*, *The Physics of Solar Cells* (PUBLISHED BY IMPERIAL COLLEGE PRESS AND DISTRIBUTED BY WORLD SCIENTIFIC PUBLISHING CO., 2003).
[17] T. Kirchartz, F. Deledalle, P. S. Tuladhar, J. R. Durrant, and J. Nelson, *On the differences between dark and light ideality factor in polymer:Fullerene solar cells*, J. Phys. Chem. Lett. **4**, 2371 (2013).
[18] O. J. Sandberg, A. Sundqvist, M. Nyman, and R. Österbacka, *Relating Charge Transport, Contact Properties, and Recombination to Open-Circuit Voltage in Sandwich-Type Thin-Film Solar Cells*, Phys. Rev. Appl. **5**, 044005 (2016).
[19] B. A. Gregg and M. C. Hanna, *Comparing organic to inorganic photovoltaic cells: Theory, experiment, and simulation*, J. Appl. Phys. **93**, 3605 (2003).
[20] C. M. Ramsdale, J. A. Barker, A. C. Arias, J. D. MacKenzie, R. H. Friend, and N. C. Greenham, *The origin of the open-circuit voltage in polyfluorene-based photovoltaic devices*, J. Appl. Phys. **92**, 4266 (2002).
[21] C. Uhrich, D. Wynands, S. Olthof, M. K. Riede, K. Leo, S. Sonntag, B. Maennig, and M. Pfeiffer, *Origin of open circuit voltage in planar and bulk heterojunction organic thin-film photovoltaics depending on doped transport layers*, J. Appl. Phys. **104**, 043107 (2008).
[22] C. J. Brabec, N. S. Sariciftci, and J. C. Hummelen, *Plastic Solar Cells*, Adv. Funct. Mater. **11**, 15 (2001).
[23] Z. He, C. Zhong, S. Su, M. Xu, H. Wu, and Y. Cao, *Enhanced power-conversion efficiency in polymer solar cells using an inverted device structure*, (2012).
[24] P. W. Bridgman, *Note on the Principle of Detailed Balancing*, Phys. Rev. **31**, 101 (1928).
[25] U. Rau, U. W. Paetzold, and T. Kirchartz, *Thermodynamics of light management in photovoltaic devices*, Phys. Rev. B - Condens. Matter Mater. Phys. **90**, 1 (2014).
[26] T. Kirchartz, U. Rau, M. Kurth, J. Mattheis, and J. H. Werner, *Comparative study of electroluminescence from Cu(In,Ga)Se2and Si solar cells*, Thin Solid Films **515**, 6238 (2007).
[27] R. T. Ross, *Some Thermodynamics of Photochemical Systems*, J. Chem. Phys. **46**, 4590 (1967).
[28] T. Kirchartz, P. Kaienburg, and D. Baran, *Figures of Merit Guiding Research on Organic Solar Cells*, J. Phys. Chem. C **122**, acs. jpcc.8b01598 (2018).
[29] U. Rau, *Reciprocity relation between photovoltaic quantum efficiency and electroluminescent emission of solar cells*, Phys. Rev. B **76**, 085303 (2007).
[30] J. Yao, T. Kirchartz, M. S. Vezie, M. A. Faist, W. Gong, Z. He, H. Wu, J. Troughton, T. Watson, D. Bryant, and J. Nelson, *Quantifying losses in open-circuit voltage in solution-processable solar cells*, Phys. Rev. Appl. **4**, 1 (2015).
[31] K. Vandewal, K. Tvingstedt, A. Gadisa, O. Inganäs, and J. V. Manca, *On the origin of the open-circuit voltage of polymer-fullerene solar cells*, Nat. Mater. **8**, 904 (2009).
[32] X. Liu, X. Du, J. J. Wang, C. Duan, X. Tang, T. Heumueller, G. Liu, Y. Li, Z. Wang, J. J. Wang, F. Liu, N. Li, C. J. Brabec, F. Huang, and Y. Cao, *Efficient Organic Solar Cells with Extremely High Open-Circuit Voltages and Low Voltage Losses by Suppressing Nonradiative Recombination Losses*, Adv. Energy Mater. **8**, 1801699 (2018).

[33] M. C. Scharber, N. A. Schultz, N. S. Sariciftci, and C. J. Brabec, *Optical- and photocurrent-detected magnetic resonance studies on conjugated polymer/fullerene composites*, Phys. Rev. B **67**, 085202 (2003).
[34] M. Zhang, H. Wang, H. Tian, Y. Geng, and C. W. Tang, *Bulk Heterojunction Photovoltaic Cells with Low Donor Concentration*, Adv. Mater. **23**, 4960 (2011).
[35] M. C. Scharber, D. Mühlbacher, M. Koppe, P. Denk, C. Waldauf, A. J. Heeger, and C. J. Brabec, *Design Rules for Donors in Bulk-Heterojunction Solar Cells—Towards 10 % Energy-Conversion Efficiency*, Adv. Mater. **18**, 789 (2006).
[36] M. Lenes, S. W. Shelton, A. B. Sieval, D. F. Kronholm, J. C. (Kees) Hummelen, and P. W. M. Blom, *Electron Trapping in Higher Adduct Fullerene-Based Solar Cells*, Adv. Funct. Mater. **19**, 3002 (2009).
[37] T. Ishwara, D. D. C. Bradley, J. Nelson, P. Ravirajan, I. Vanseveren, T. Cleij, D. Vanderzande, L. Lutsen, S. Tierney, M. Heeney, and I. McCulloch, *Influence of polymer ionization potential on the open-circuit voltage of hybrid polymer/TiO2 solar cells*, Appl. Phys. Lett. **92**, 053308 (2008).
[38] V. D. Mihailetchi, P. W. M. Blom, J. C. Hummelen, and M. T. Rispens, *Cathode dependence of the open-circuit voltage of polymer:fullerene bulk heterojunction solar cells*, J. Appl. Phys. **94**, 6849 (2003).
[39] R. Xia, D.-S. Leem, T. Kirchartz, S. Spencer, C. Murphy, Z. He, H. Wu, S. Su, Y. Cao, J. S. Kim, J. C. deMello, D. D. C. Bradley, and J. Nelson, *Investigation of a Conjugated Polyelectrolyte Interlayer for Inverted Polymer:Fullerene Solar Cells*, Adv. Energy Mater. **3**, 718 (2013).
[40] S. Wheeler, F. Deledalle, N. Tokmoldin, T. Kirchartz, J. Nelson, and J. R. Durrant, *Influence of Surface Recombination on Charge-Carrier Kinetics in Organic Bulk Heterojunction Solar Cells with Nickel Oxide Interlayers*, Phys. Rev. Appl. **4**, 29 (2015).
[41] A. Maurano, R. Hamilton, C. G. Shuttle, A. M. Ballantyne, J. Nelson, B. O'Regan, W. Zhang, I. McCulloch, H. Azimi, M. Morana, C. J. Brabec, J. R. Durrant, B. O'Regan, W. Zhang, I. McCulloch, H. Azimi, M. Morana, C. J. Brabec, and J. R. Durrant, *Recombination dynamics as a key determinant of open circuit voltage in organic bulk heterojunction solar cells: A comparison of four different donor polymers*, Adv. Mater. **22**, 4987 (2010).
[42] S. D. Collins, C. M. Proctor, N. A. Ran, and T.-Q. Nguyen, *Understanding Open-Circuit Voltage Loss through the Density of States in Organic Bulk Heterojunction Solar Cells*, Adv. Energy Mater. **6**, 1501721 (2016).
[43] S. Chen, S.-W. W. Tsang, T.-H. H. Lai, J. R. Reynolds, and F. So, *Dielectric effect on the photovoltage loss in organic photovoltaic cells*, Adv. Mater. **26**, 6125 (2014).
[44] K. Vandewal, J. Widmer, T. Heumueller, C. J. Brabec, M. D. McGehee, K. Leo, M. Riede, and A. Salleo, *Increased Open-Circuit Voltage of Organic Solar Cells by Reduced Donor-Acceptor Interface Area*, Adv. Mater. **26**, 3839 (2014).
[45] R. A. Street, D. Davies, P. P. Khlyabich, B. Burkhart, and B. C. Thompson, *Origin of the Tunable Open-Circuit Voltage in Ternary Blend Bulk Heterojunction Organic Solar Cells*, (2013).
[46] M. C. Scharber, D. Mühlbacher, M. Koppe, P. Denk, C. Waldauf, A. J. Heeger, and C. J. Brabec, *Design Rules for Donors in Bulk-Heterojunction Solar Cells—Towards 10 % Energy-Conversion Efficiency*, Adv. Mater. **18**, 789 (2006).
[47] J. Benduhn, K. Tvingstedt, F. Piersimoni, S. Ullbrich, Y. Fan, M. Tropiano, K. A. McGarry, O. Zeika, M. K. Riede, C. J. Douglas, S. Barlow, S. R. Marder, D. Neher, D. Spoltore, and K. Vandewal, *Intrinsic non-radiative voltage losses in fullerene-based organic solar cells*, Nat. Energy **2**, 17053 (2017).
[48] J. Liu, S. Chen, D. Qian, B. Gautam, G. Yang, J. Zhao, J. Bergqvist, F. Zhang, W. Ma, H. Ade, O. Inganäs, K. Gundogdu, F. Gao, and H. Yan, *Fast charge separation in a non-fullerene organic solar cell with a small driving force*, Nat. Energy **1**, 16089 (2016).
[49] Y. Cui, C. Yang, H. Yao, J. Zhu, Y. Wang, G. Jia, F. Gao, and J. Hou, *Efficient Semitransparent Organic Solar Cells with Tunable Color enabled by an Ultralow-Bandgap Nonfullerene Acceptor*, Adv. Mater. **29**, 1 (2017).
[50] D. Veldman, S. C. J. Meskers, and R. A. J. Janssen, *The energy of charge-transfer states in electron donor-acceptor blends: insight into the energy losses in organic solar cells*, Adv. Funct. Mater. **19**, 1939 (2009).
[51] M. A. Faist, T. Kirchartz, W. Gong, R. S. Ashraf, I. McCulloch, J. C. De Mello, N. J. Ekins-Daukes, D. D. C. Bradley, and J. Nelson, *Competition between the charge transfer state and the singlet states of donor or acceptor limiting the efficiency in polymer: Fullerene solar cells*, J. Am. Chem. Soc. **134**, 685 (2012).
[52] L. Goris, K. Haenen, M. Nesládek, P. Wagner, D. Vanderzande, L. De Schepper, J. D'haen, L. Luisen, and J. V. Manca, *Absorption phenomena in organic thin films for solar cell applications investigated by photothermal deflection spectroscopy*, J. Mater. Sci. **40**, 1413 (2005).
[53] U. Hörmann, J. Kraus, M. Gruber, C. Schuhmair, T. Linderl, S. Grob, S. Kapfinger, K. Klein, M.

Stutzman, H. J. Krenner, and W. Brütting, *Quantification of energy losses in organic solar cells from temperature-dependent device characteristics*, Phys. Rev. B **88**, 235307 (2013).
[54] Z. Fei, F. D. Eisner, X. Jiao, M. Azzouzi, J. A. Röhr, Y. Han, M. Shahid, A. S. R. Chesman, C. D. Easton, C. R. McNeill, T. D. Anthopoulos, J. Nelson, and M. Heeney, *An Alkylated Indacenodithieno[3,2- b]thiophene-Based Nonfullerene Acceptor with High Crystallinity Exhibiting Single Junction Solar Cell Efficiencies Greater than 13% with Low Voltage Losses*, Adv. Mater. 1705209 (2018).
[55] U. Rau, B. Blank, T. C. M. Müller, and T. Kirchartz, *Efficiency Potential of Photovoltaic Materials and Devices Unveiled by Detailed-Balance Analysis*, Phys. Rev. Appl. **7**, 044016 (2017).
[56] C. Wang, X. Xu, W. Zhang, J. Bergqvist, Y. Xia, X. Meng, K. Bini, W. Ma, A. Yartsev, K. Vandewal, M. R. Andersson, O. Inganäs, M. Fahlman, and E. Wang, *Low Band Gap Polymer Solar Cells With Minimal Voltage Losses*, Adv. Energy Mater. **6**, 1600148 (2016).
[57] H. Fu, Y. Wang, D. Meng, Z. Ma, Y. Li, F. Gao, Z. Wang, and Y. Sun, *Suppression of Recombination Energy Losses by Decreasing the Energetic Offsets in Perylene Diimide-Based Nonfullerene Organic Solar Cells*, {ACS} Energy Lett. **3**, 2729 (2018).
[58] S. Xie, Y. Xia, Z. Zheng, X. Zhang, J. Yuan, H. Zhou, and Y. Zhang, *Effects of Nonradiative Losses at Charge Transfer States and Energetic Disorder on the Open-Circuit Voltage in Nonfullerene Organic Solar Cells*, Adv. Funct. Mater. **28**, 1705659 (2017).
[59] T. Li, J. Benduhn, Y. Li, F. Jaiser, D. Spoltore, O. Zeika, Z. Ma, D. Neher, K. Vandewal, and K. Leo, *Boron dipyrromethene ({BODIPY}) with meso-perfluorinated alkyl substituents as near infrared donors in organic solar cells*, J. Mater. Chem. A **6**, 18583 (2018).
[60] M. E. Ziffer, S. Byeok Jo, H. Zhong, L. Ye, H. Liu, F. Lin, J. Zhang, X. Li, H. W. Ade, A. K-Y Jen, D. S. Ginger, H. Kong, S. B. Jo, H. Zhong, L. Ye, H. Liu, F. Lin, J. Zhang, X. Li, H. W. Ade, A. K.-Y. Jen, D. S. Ginger, S. Byeok Jo, H. Zhong, L. Ye, H. Liu, F. Lin, J. Zhang, X. Li, H. W. Ade, A. K-Y Jen, and D. S. Ginger, *Long-Lived, Non-Geminate, Radiative Recombination of Photogenerated Charges in a Polymer/Small-Molecule Acceptor Photovoltaic Blend*, J. Am. Chem. Soc. **140**, 9996 (2018).
[61] L. C. W. de Menezes, Y. Jin, L. Benatto, C. Wang, M. Koehler, F. Zhang, and L. S. Roman, *Charge Transfer Dynamics and Device Performance of Environmentally Friendly Processed Nonfullerene Organic Solar Cells*, {ACS} Appl. Energy Mater. **1**, 4776 (2018).
[62] W. Deng, K. Gao, J. Yan, Q. Liang, Y. Xie, Z. He, H. Wu, X. Peng, and Y. Cao, *Origin of Reduced Open-Circuit Voltage in Highly Efficient Small-Molecule-Based Solar Cells upon Solvent Vapor Annealing*, {ACS} Appl. Mater. Interfaces **10**, 8141 (2018).
[63] J. Zhang, B. Kan, A. J. Pearson, A. J. Parnell, J. F. K. Cooper, X.-K. Liu, P. J. Conaghan, T. R. Hopper, Y. Wu, X. Wan, F. Gao, N. C. Greenham, A. A. Bakulin, Y. Chen, and R. H. Friend, *Efficient non-fullerene organic solar cells employing sequentially deposited donor{\textendash}acceptor layers*, J. Mater. Chem. A **6**, 18225 (2018).
[64] Z. Zhou, S. Xu, J. Song, Y. Jin, Q. Yue, Y. Qian, F. Liu, F. Zhang, and X. Zhu, *High-efficiency small-molecule ternary solar cells with a hierarchical morphology enabled by synergizing fullerene and non-fullerene acceptors*, Nat. Energy **3**, 952 (2018).
[65] D. Baran, T. Kirchartz, S. Wheeler, S. Dimitrov, M. Abdelsamie, J. Gorman, R. S. Ashraf, S. Holliday, A. Wadsworth, N. Gasparini, P. Kaienburg, H. Yan, A. Amassian, C. J. Brabec, J. R. Durrant, and I. McCulloch, *Reduced voltage losses yield 10% efficient fullerene free organic solar cells with $\greater$1 V open circuit voltages*, Energy Environ. Sci. **9**, 3783 (2016).
[66] V. C. Nikolis, J. Benduhn, F. Holzmueller, F. Piersimoni, M. Lau, O. Zeika, D. Neher, C. Koerner, D. Spoltore, and K. Vandewal, *Reducing Voltage Losses in Cascade Organic Solar Cells while Maintaining High External Quantum Efficiencies*, Adv. Energy Mater. **7**, 1700855 (2017).
[67] S. Chen, Y. Wang, L. Zhang, J. Zhao, Y. Chen, D. Zhu, H. Yao, G. Zhang, W. Ma, R. H. Friend, P. C. Y. Chow, F. Gao, and H. Yan, *Efficient Nonfullerene Organic Solar Cells with Small Driving Forces for Both Hole and Electron Transfer*, Adv. Mater. **30**, 1804215 (2018).
[68] D. Yang, Y. Wang, T. Sano, F. Gao, H. Sasabe, and J. Kido, *A minimal non-radiative recombination loss for efficient non-fullerene all-small-molecule organic solar cells with a low energy loss of 0.54~{eV} and high open-circuit voltage of 1.15 V*, J. Mater. Chem. A **6**, 13918 (2018).
[69] D. Qian, Z. Zheng, H. Yao, W. Tress, T. R. Hopper, S. Chen, S. Li, J. Liu, S. Chen, J. Zhang, X.-K. Liu, B. Gao, L. Ouyang, Y. Jin, G. Pozina, I. A. Buyanova, W. M. Chen, O. Inganäs, V. Coropceanu, J.-L. Bredas, H. Yan, J. Hou, F. Zhang, A. A. Bakulin, and F. Gao, *Design rules for minimizing voltage losses in high-efficiency organic solar cells*, Nat. Mater. **17**, 703 (2018).
[70] L. Zhan, S. Li, H. Zhang, F. Gao, T.-K. Lau, X. Lu, D. Sun, P. Wang, M. Shi, C.-Z. Li, and H. Chen, *A Near-Infrared Photoactive Morphology Modifier Leads to Significant Current Improvement and Energy Loss Mitigation for Ternary Organic Solar Cells*, Adv. Sci. **5**, 1800755 (2018).
[71] W. Shockley and H. Queisser, *Detailed balance limit of efficiency of p-n junction solar cells*, J. Appl.

Phys. **32**, 510 (1961).
[72] S. Ko, E. T. Hoke, L. Pandey, S. Hong, R. Mondal, C. Risko, Y. Yi, R. Noriega, M. D. McGehee, J.-L. Brédas, A. Salleo, and Z. Bao, *Controlled Conjugated Backbone Twisting for an Increased Open-Circuit Voltage while Having a High Short-Circuit Current in Poly(hexylthiophene) Derivatives*, J. Am. Chem. Soc. **134**, 5222 (2012).
[73] J. Hou, O. Inganäs, R. H. Friend, and F. Gao, *Organic solar cells based on non-fullerene acceptors*, Nat. Mater. **17**, 119 (2018).
[74] C.-C. Lee, W.-C. Su, and W.-C. Chang, *Effects of the charge-transfer reorganization energy on the open-circuit voltage in small-molecular bilayer organic photovoltaic devices: comparison of the influence of deposition rates of the donor*, Phys. Chem. Chem. Phys. **18**, 12651 (2016).
[75] T. M. Burke, S. Sweetnam, K. Vandewal, and M. D. McGehee, *Beyond Langevin recombination: How equilibrium between free carriers and charge transfer states determines the open-circuit voltage of organic solar Cells*, Adv. Energy Mater. **5**, 1 (2015).
[76] S. M. Tuladhar, M. Azzouzi, F. Delval, J. Yao, A. A. Y. Guilbert, T. Kirchartz, N. F. Montcada, R. Dominguez, F. Langa, E. Palomares, and J. Nelson, *Low Open-Circuit Voltage Loss in Solution-Processed Small-Molecule Organic Solar Cells*, ACS Energy Lett. **1**, 302 (2016).
[77] S. Few, J. M. Frost, J. Kirkpatrick, and J. Nelson, *Influence of Chemical Structure on the Charge Transfer State Spectrum of a Polymer:Fullerene Complex*, J. Phys. Chem. C **118**, 8253 (2014).
[78] X. Liu, K. Ding, A. Panda, and S. R. Forrest, *Charge Transfer States in Dilute Donor-Acceptor Blend Organic Heterojunctions*, ACS Nano **10**, 7619 (2016).
[79] F. Piersimoni, S. Chambon, K. Vandewal, R. Mens, T. Boonen, A. Gadisa, M. Izquierdo, S. Filippone, B. Ruttens, J. D'haen, N. Martin, L. Lutsen, D. Vanderzande, P. Adriaensens, and J. V. Manca, *Influence of fullerene ordering on the energy of the charge-transfer state and open-circuit voltage in polymer:fullerene solar cells*, J. Phys. Chem. C **115**, 10873 (2011).
[80] K. R. Graham, C. Cabanetos, J. P. Jahnke, M. N. Idso, A. El Labban, G. O. Ngongang Ndjawa, T. Heumueller, K. Vandewal, A. Salleo, B. F. Chmelka, A. Amassian, P. M. Beaujuge, M. D. Mcgehee, S. Arabia, A. El Labban, G. O. Ngongang Ndjawa, T. Heumueller, K. Vandewal, A. Salleo, B. F. Chmelka, A. Amassian, P. M. Beaujuge, and M. D. Mcgehee, *Importance of the Donor:Fullerene intermolecular arrangement for high-efficiency organic photovoltaics*, J. Am. Chem. Soc. **136**, 9608 (2014).
[81] K. Vandewal, S. Albrecht, E. T. Hoke, K. R. Graham, J. Widmer, J. D. Douglas, M. Schubert, W. R. Mateker, J. T. Bloking, G. F. Burkhard, A. Sellinger, J. M. J. Fréchet, A. Amassian, M. K. Riede, M. D. McGehee, D. Neher, and A. Salleo, *Efficient charge generation by relaxed charge-transfer states at organic interfaces*, Nat. Mater. **13**, 63 (2013).
[82] Y. Li, X. Liu, F.-P. Wu, Y. Zhou, Z.-Q. Jiang, B. Song, Y. Xia, Z.-G. Zhang, F. Gao, O. Inganäs, Y. Li, and L.-S. Liao, *Non-fullerene acceptor with low energy loss and high external quantum efficiency: towards high performance polymer solar cells*, J. Mater. Chem. A **4**, 5890 (2016).
[83] Z. Liu, L. Krückemeier, B. Krogmeier, B. Klingebiel, J. A. Márquez, S. Levcenko, S. Öz, S. Mathur, U. Rau, T. Unold, and T. Kirchartz, *Open-Circuit Voltages Exceeding 1.26 V in Planar Methylammonium Lead Iodide Perovskite Solar Cells*, ACS Energy Lett. **4**, 110 (2019).
[84] C. Deibel, A. Wagenpfahl, and V. Dyakonov, *Origin of reduced polaron recombination in organic semiconductor devices*, Phys. Rev. B - Condens. Matter Mater. Phys. **80**, 1 (2009).
[85] D. Bartesaghi, I. del C. Pérez, J. Kniepert, S. Roland, M. Turbiez, D. Neher, and L. J. A. Koster, *Competition between recombination and extraction of free charges determines the fill factor of organic solar cells*, Nat. Commun. **6**, 7083 (2015).
[86] C. Göhler, A. Wagenpfahl, and C. Deibel, *Nongeminate Recombination in Organic Solar Cells*, Adv. Electron. Mater. 1700505 (2018).
[87] M. Azzouzi, J. Yan, T. Kirchartz, K. Liu, J. Wang, H. Wu, and J. Nelson, *Nonradiative Energy Losses in Bulk-Heterojunction Organic Photovoltaics*, Phys. Rev. X **8**, (2018).
[88] X. K. Chen and J. L. Brédas, *Voltage Losses in Organic Solar Cells: Understanding the Contributions of Intramolecular Vibrations to Nonradiative Recombinations*, Adv. Energy Mater. **8**, 1 (2018).
[89] I. R. Gould, D. Noukakis, J. L. Goodman, R. H. Young, and S. Farid, *A Quantitative Relationship between Radiative and Nonradiative Electron Transfer in Radical-Ion Pairs*, Chem. Phys. **176**, 439 (1993).
[90] G. D. ' Avino, L. Muccioli, Y. Olivier, and D. Beljonne, *Charge Separation and Recombination at Polymer−Fullerene Heterojunctions: Delocalization and Hybridization Effects*, J. Phys. Chem. Lett **7**, 12 (2016).
[91] C. J. Brabec, M. Heeney, I. McCulloch, and J. Nelson, *Influence of blend microstructure on bulk heterojunction organic photovoltaic performance*, Chem. Soc. Rev. **40**, 1185 (2011).
[92] M. C. Scharber and N. S. Sariciftci, *Efficiency of bulk-heterojunction organic solar cells*, Prog. Polym.

Sci. **38**, 1929 (2013).
[93] R. A. J. Janssen and J. Nelson, *Factors limiting device efficiency in organic photovoltaics*, Adv. Mater. **25**, 1847 (2013).
[94] K. Vandewal, Z. Ma, J. Bergqvist, Z. Tang, E. Wang, P. Henriksson, K. Tvingstedt, M. R. Andersson, F. Zhang, and O. Inganäs, *Quantification of Quantum Efficiency and Energy Losses in Low Bandgap Polymer:Fullerene Solar Cells with High Open-Circuit Voltage*, Adv. Funct. Mater. **22**, 3480 (2012).
[95] N. A. Ran, J. A. Love, C. J. Takacs, A. Sadhanala, J. K. Beavers, S. D. Collins, Y. Huang, M. Wang, R. H. Friend, G. C. Bazan, and T.-Q. Nguyen, *Harvesting the Full Potential of Photons with Organic Solar Cells*, Adv. Mater. **28**, 1482 (2016).
[96] E. R. Bittner and C. Silva, *Noise-induced quantum coherence drives photo-carrier generation dynamics at polymeric semiconductor heterojunctions.*, Nat. Commun. **5**, 3119 (2014).
[97] S. N. Hood and I. Kassal, *Entropy and Disorder Enable Charge Separation in Organic Solar Cells*, J. Phys. Chem. Lett. **7**, 4495 (2016).
[98] W. Gao, T. Liu, C. Zhong, G. Zhang, Y. Zhang, R. Ming, L. Zhang, J. Xin, K. Wu, Y. Guo, W. Ma, H. Yan, Y. Liu, and C. Yang, *Asymmetrical Small Molecule Acceptor Enabling Nonfullerene Polymer Solar Cell with Fill Factor Approaching 79%*, **16**, 10 (2018).
[99] S. A. Haque, E. Palomares, B. M. Cho, A. N. M. Green, N. Hirata, D. R. Klug, and J. R. Durrant, *Charge Separation versus Recombination in Dye-Sensitized Nanocrystalline Solar Cells: the Minimization of Kinetic Redundancy*, J. Am. Chem. Soc. **127**, 3456 (2005).
[100] F. Gao, W. Tress, J. Wang, and O. Inganäs, *Temperature dependence of charge carrier generation in organic photovoltaics*, Phys. Rev. Lett. **114**, 1 (2015).
[101] A. N. Bartynski, M. Gruber, S. Das, S. Rangan, S. Mollinger, C. Trinh, S. E. Bradforth, K. Vandewal, A. Salleo, R. A. Bartynski, W. Bruetting, and M. E. Thompson, *Symmetry-Breaking Charge Transfer in a Zinc Chlorodipyrrin Acceptor for High Open Circuit Voltage Organic Photovoltaics*, J. Am. Chem. Soc. **137**, 5397 (2015).

GLOSSARY

Bimolecular recombination: Recombination of an electron and hole where that charge carriers need to find each other before recombining. The process is rate-limited by the charge carriers meeting and the rate depends on the population of each carrier type that is available for recombination. Direct band-to-band recombination is an example of bimolecular recombination.

Charge Transfer (CT) state: is an excited state that extends over two or more molecules such that the participating molecules carry a different net charge. In donor: acceptor complexes as at the heterojunction in OPV devices, the state extends over donor and acceptor with a large fraction of the electronic charge transferred to the acceptor molecule(s) from the donor. Such a state may also be referred to as a "bound state" at the interface between the donor and the acceptor media.

Charge Transfer state energy (E_{CT}): the energy, relative to the ground state, of the lowest charge transfer state in a donor: acceptor system.

Effective density of states in the conduction band (N_c) or in the valence band (N_v): the density of available states for the electron above the conduction band minimum energy, or for the hole below the valence band maximum energy. These terms normally apply to crystalline inorganic semiconductors. For charge densities in organic semiconductors the appropriate quantity would be the density of electron transporting orbitals or hole transporting orbitals energetically accessible to the charge carrier.

Electroluminescence spectroscopy (EL): A characterisation technique that measures the luminescence of a solar cell, or other device equipped with electron and hole injecting contacts, when an electric current is passed through it. It is commonly used to characterise the optical properties of the lowest energy state in a photovoltaic device.

Excess loss due to the non-sharp absorption onset ($\Delta V_{oc,abs}$): Difference between the open-circuit voltage in the radiative limit calculated for an external quantum efficiency (EQE) spectrum that turns on sharply at the band gap (as in the Shockley-Queisser limit)), $V_{oc,SQ}$ and the open-circuit voltage in the radiative limit calculated for the EQE spectrum measured on a device $V_{oc,rad}$.

Excess non-radiative voltage losses ($\Delta V_{oc,nrad}$): Difference between the radiative limit to the open-circuit voltage of a device, $V_{oc,rad}$, calculated as above, and the actual measured open-circuit voltage of the device.

Exciton state: An excited state in which the electron and electron hole are localised in the same region of space, attracted to each other by the electrostatic Coulomb force. The exciton can be considered as a single entity, with a well-defined spin of 0 (for a singlet exciton) or 1 (for a triplet). Unlike the CT state, an exciton is normally charge-neutral over space.

External luminescence quantum efficiency (Q_e^{lum}): Ratio of the number of externally observed photons to the number of injected charge carriers that lead to the luminescence. This efficiency combines the outcoupling efficiency of the light and the ratio of the radiative recombination current to the overall recombination current.

Heterojunction: an interface between two semiconductor materials with different energy levels, that sets up a step in the energy profile as seen by electrons and / or holes, usually driving the electrons to one side and the holes to the other. In organic solar cells, 'bulk heterojunction' refers to a mixture (rather than two flat layers) of two such organic semiconductors.

Highest occupied molecular orbital (HOMO): The highest energy molecular orbital that is occupied by an electron. The HOMO energy is often considered analogous to the valence band in semiconductor physics.

Ideality factor (n_{id}): A measure to characterise how closely a device follows ideal solar cell behaviour. In the general case, recombination current R depends on applied voltage V like $R \propto e^{qV/n_{id}kT}$ where q, k and T refer to electronic charge, Boltzmann's constant and temperature and n_{id} quantifies the deviation from ideal behaviour, $R \propto e^{qV/kT}$. The value of n_{id} can be interpreted in terms of the dominant recombination mechanism.

Interfacial band gap (E_i): An energy used in bulk heterojunction devices to refer to the effective electrical band gap at the interface that is provided by the LUMO, or conduction band, of the electron-accepting side and the HOMO, or valence band, of the electron-donating side. The interfacial gap will generally be smaller than the band gap of either heterojunction component alone.

Interfacial offset (E_g-E_i or $E_{L,A}$ - $E_{H,D}$): The offset in energy at the donor/acceptor interface, quantified usually as whichever of the differences, in LUMO energy or HOMO energy, is the lower. This offset provides a driving energy for charge transfer across the interface and is commonly considered necessary to enable efficient separation of the photo-excited exciton into independent charges. The interfacial offset energy is measured in different ways depending on the model considered.

Lowest unoccupied molecular orbital (LUMO): The lowest energy molecular orbital that is unoccupied by an electron. The LUMO energy is often considered analogous to the conduction band in semiconductor physics.

Non-fullerene acceptors (NFAs): A molecular acceptor that is not based on the very widely used C60 and C70 fullerene molecules.

Non-Radiative recombination: Recombination of an electron and hole that does not result in the emission of a photon. This type of recombination is an avoidable loss mechanism that, unlike radiative recombination, can theoretically be avoided.

Open circuit voltage (V_{oc}): Voltage of the cell under light irradiance when no current is flowing through the cell and the terminals are isolated from each other. It corresponds to the voltage at which the overall generation rate in the cell is equal to the overall recombination rate. Voc is usually quoted under a standard (Ar Mass 1.5, intensity 1000 W m^{-2}) solar irradiance

Optical band gap (E_g): For a perfect semiconductor it refers to the energy above which a photon can be absorbed**.** However, for material as disordered as OPV, The band gap is not properly defined therefore the optical band gap value depends on assumptions made to model the material as a perfect semiconductor.

Organic photovoltaic (OPV): A type of photovoltaic that uses organic semiconductors as the light absorbing and charge transporting components.

Power conversion efficiency (PCE): The efficiency of a solar cell measured as the output electrical power divided by the total radiant energy incident on the device from the illuminating light source (usually the standard solar irradiance of 1000W m^{-2}).

Quasi-Fermi levels: a measure of the population of charge carriers (either electrons or holes) at a point in a semiconductor relative to the population of the same charge carrier in the relevant (conduction or valence) band of the material at equilibrium. The quasi Fermi energy is defined as kT times the natural logarithm of that ratio of charge densities, and can be compared with the band edges in an analogous way to the Fermi level of a system at equilibrium.

Radiative open-circuit voltage ($V_{oc,rad}$): Value of the theoretical open-circuit voltage of a solar cell in the radiative limit, calculated using the reciprocity principle and the measured EQE of the device.

Radiative recombination: Recombination of an electron and hole that results in the emission of a photon. Such recombination events are unavoidable in solar cells due to the reciprocity of light absorption and light emission.

Shockley Queisser Limit open circuit voltage ($V_{oc,SQ}$) : Value of the theoretical open-circuit voltage of a solar cell in the radiative limit, calculated using the reciprocity principle and the band gap E_g of the absorber. For this purpose the absorption of the cell is considered a step function where no photon is absorbed lower than E_g and all the photons higher than E_g generate charges.

Short circuit current density (Jsc): the electric current density delivered by a solar cell under short circuit conditions and standard solar irradiance.

The principle of reciprocity: This refers to the reciprocity between light absorption and light emission by a semiconductor, embodied in Einstein coefficients that relate absorption and emission, and an equivalent reciprocal relationship between the electroluminescence spectrum of a solar cell and its external quantum efficiency spectrum. This reciprocity is the basis of the solar cell efficiency limit introduced by Shockley and Queisser.